WATER RESOURCES RESEARCH, VOL. 31, NO. 6, PAGES 1595–1605, JUNE 1995

Nonperiodic eddy pulsations

D. M. Rubin and R. R. McDonald[1]
U.S. Geological Survey, Menlo Park, California

Abstract. Recirculating flow in lateral separation eddies is typically weaker than main stem flow and provides an effective environment for trapping sediment. Observations of recirculating flow and sedimentary structures demonstrate that eddies pulsate in size and in flow velocity even when main stem flow is steady. Time series measurements of flow velocity and location of the reattachment point indicate that these pulsations are nonperiodic. Nonperiodic flow in the lee of a channel margin constriction is grossly different from the periodic flow in the lee of a cylinder that is isolated in a flow. Our experiments demonstrate that placing a flow-parallel plate adjacent to a cylinder is sufficient to cause the leeside flow to change from a periodic sequence of vortices to a nonperiodically pulsating lateral separation eddy, even if flow conditions are otherwise unchanged. Two processes cause the leeside flow to become nonperiodic when the plate is added. First, vortices that are shed from the cylinder deform and become irregular as they impact the plate or interfere with remnants of other vortices near the reattachment point. Second, these deformed vortices and other flow structures are recirculated in the lateral separation eddy, thereby influencing the future state (pressure and momentum distribution) of the recirculating flow. The vortex deformation process was confirmed experimentally by documenting spatial differences in leeside flow; vortex shedding that is evident near the separation point is undetectable near the reattachment point. Nonlinear forecasting techniques were used in an attempt to distinguish among several possible kinds of nonperiodic flows. The computational techniques were unable to demonstrate that any of the nonperiodic flows result from low-dimensional nonlinear processes.

Introduction

Purpose

The purpose of this paper is to document, characterize, and attempt to explain the origin of irregularly pulsating flow in lateral separation eddies; previous hydrologic and sedimentologic work has largely ignored this property of recirculating flow. This study began with field observations of sedimentary structures (oscillation ripples), which showed that lateral separation eddies pulsate even when main stem flow is steady. The field situation, however, is complicated in geometry (irregular banks and a wide range of roughness elements), is possibly affected by wind, and exists at high Reynolds number. To minimize these complexities, we used data from laboratory lateral separation eddies. One set of lab data was from such a large flume (4 m width) that the flume can be thought of as a creek or small river (see *Schmidt et al.* [1993] for a description of the flume and related recirculation experiments). The second set of data was collected in a very small flume and was not an attempt to model natural rivers; rather it was an experiment to see if a grossly oversimplified system (well-regulated main stem flow, extremely simple channel geometry, and relatively low Reynolds number) would retain the pulsating behavior observed in the field and large flume. Finally, we used spectral analysis and nonlinear forecasting to characterize the observed flows and to help explain the origin of the observed pulsations.

[1]Now at U.S. Geological Survey, Denver, Colorado.

This paper is not subject to U.S. copyright. Published in 1995 by the American Geophysical Union.

Paper number 95WR00472.

Background

Flow separation, recirculation, and reattachment occur in virtually all fluvial channels, wherever the bed or bank bends too abruptly for the flow to follow (Figure 1). Because the relatively weak flow within and adjacent to recirculation zones is a prime site for deposition, recirculation processes are fundamental in reducing or eliminating bank irregularities and in controlling the morphology of alluvial channels [*Leopold et al.*, 1960; *Leeder and Bridges*, 1975]. Recirculating flow also has been recognized as an important control of deposition in bedrock channels [*Rubin et al.*, 1990; *Schmidt*, 1990; *Schmidt and Graf*, 1990; *Andrews*, 1991; *Nelson*, 1991; *Schmidt et al.*, 1993].

Most hydraulic studies of lateral separation eddies in rivers have been directed at generalizing mean flow properties [*Yeh et al.*, 1988] or characterizing periodic behavior resulting from vortex shedding, but a number of studies [*Cherry et al.*, 1984; *Driver et al.*, 1987; *Simpson*, 1989] have documented the nonperiodic behavior of flow within separation eddies, even in experiments where flow from upstream is steady. Although steady flow models [*Andrews*, 1991; *Nelson*, 1991; *Nelson et al.*, 1994; *Smith and Wiele*, 1994] may prove sufficient for generalizing the mean flow and depositional rates within lateral separation eddies, the nonperiodic pulsations are nevertheless an intrinsic property of eddies. The large-scale depositional effects of these pulsations are unknown, but on a small and easily observable scale, the pulsations have a demonstrable effect: They produce ripples that resemble wave-generated ripples [*Rubin*, 1987; *Rubin et al.*, 1990; *Schmidt et al.*, 1993]. These symmetrical, reversing, eddy pulsation ripples are common near the reattachment point on sandbars in bedrock canyons and also occur near the reattachment point on bends in sand-

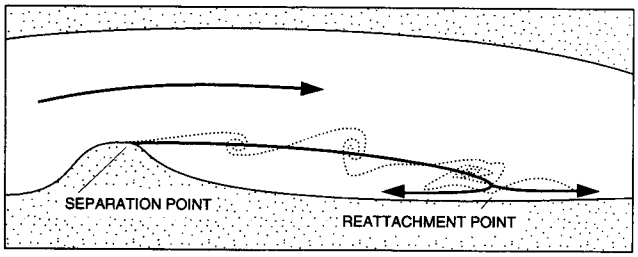

Figure 1. Schematic planform diagram showing a recirculation zone in a river channel expansion; vortex structure is schematic.

bed channels (*Rubin et al.*'s [1990] interpretation of Mississippi River structures shown by *Davies* [1966, plates 1B and 1C]).

Sedimentologists recognize two main classes of ripples: current ripples (those that form in currents that are unimodal in direction) and oscillation ripples (those that form in reversing currents such as waves). "Oscillation" ripples also form without waves in the reversing flows that occur where separated flow reattaches to the bed or bank at the downstream end of an eddy. Ripples have been hypothesized to form by such reversing flows downstream from obstacles on the seafloor [*Shipek*, 1962] and have been observed to form in lateral separation eddies in rivers [*Rubin*, 1987; *Rubin et al.*, 1990; *Schmidt et al.*, 1993]. Recognition of these ripples in recirculating eddies was the first documentation that eddy pulsations affect sediment transport in rivers.

Our initial hypothesis was that the oscillation ripples were produced by vortex-induced oscillating flow. We hypothesized that each vortex that was shed from the separation point might cause upstream flow when its leading side impacted the bank in the reattachment zone, followed by downstream flow when its trailing edge hit the bank, essentially the same process as that by which the circulation of cyclonic weather systems causes a rotation in wind direction with the passage of a storm. Visual inspection of the flow could not detect such a regular succession of vortices impacting the bank, and, as measurements were to demonstrate later, flow in the zone of reattaching flow is dominated by nonperiodic upstream-downstream flow reversals; these reversals are caused by changes in location of the instantaneous reattachment point, a process that alternately incorporates or excludes points in the reattachment zone from the recirculating flow in the eddy. As will be shown below, these pulsations arise spontaneously even where main stem flow is steady.

Hypotheses for Eddy Nonperiodicity

The problem of eddy nonperiodicity can be illustrated by considering two flow examples. One example is the complicated nonperiodic flow that occurs in lateral separation eddies behind obstacles along riverbanks. The other example is the periodic sequence of vortices (vortex street) shed in the lee of a cylinder in a laboratory flume [*Schlichting*, 1968]. There are many differences between these two flow situations: Flow in a river typically has a higher Reynolds number than ideal vortex streets in the lab; riverbanks are sloping, they are rougher, and they have a wide variety of roughness scales; constrictions in rivers are geometrically more complex than a cylinder; and riverbank constrictions occur at the margins of the flow, whereas vortex streets occur in the lee of isolated obstacles. Because of these many differences, it is impossible to attribute the nonperiodicity of lateral separation eddies to any single cause without conducting experiments such as those described below. In this study we test the hypothesis that placing an obstacle such as a cylinder adjacent to a smooth wall is sufficient to cause the leeside flow to change from a periodic vortex street to a nonperiodically pulsating eddy.

General Causes of Periodicity and Nonperiodicity

Periodic behavior of a system can result either from periodic external forcing (for example, periodic variations in sediment transport that occur in response to periodic tidal currents) or from intrinsic response to steady forcing (periodic tides that form in response to steady orbital forcing). Similarly, nonperiodicity can result from the same two causes: external forcing or intrinsic behavior. It is easy to understand how unsteady external forcing (such as unsteady main stem discharge or unsteady wind-driven circulation within eddies) might cause nonperiodicity. But nonperiodicity can also result from intrinsic behaviors, even where forcing is steady or periodic. Intrinsic nonperiodic behavior can arise both in low-dimensional deterministic systems with only a few degrees of freedom (chaos such as *Lorenz*'s [1963] convection cells) and in high-dimensional stochastic systems with a large number of degrees of freedom (motion of a molecule in a volume of gas). In the former case the system has few degrees of freedom, but each time it returns to conditions that are nearly similar (but not exactly similar) it evolves differently; nonperiodicity results from this sensitive behavior. In the latter case the system is nonperiodic because it has so many degrees of freedom that it does not return to initial conditions that are even approximately similar.

One of the goals of this investigation is to characterize the origin of nonperiodic eddy pulsations. Our approach is to show that the nonperiodicity occurs even where external forcing is constant, thereby demonstrating that nonperiodicity is intrinsic to the system. The next step is to determine whether this nonperiodicity results from low-dimensional determinism (chaos) or high-dimensional processes.

Several techniques have been used successfully to document the role of chaos in weakly turbulent flows such as Couette cylinder flow or convection rolls [*Gollub and Swinney*, 1975; *Gollub et al.*, 1980]. In general, experimental conditions must be only weakly turbulent, transitional between periodic and nonperiodic (turbulent). In previous experiments this has been accomplished by adjusting the Reynolds or Prandtl number. Time series are then recorded at a point in the fluid and are examined for period doubling, intermittency, or other properties that are characteristic of chaos. In the present experiments an abrupt transition to turbulence is induced not by changing the Reynolds number, but rather by making a single change to the geometry of the flow.

Methods

Observational Techniques

Field observations of ripples and eddy pulsations were conducted in the Colorado River in Grand Canyon. Detailed descriptions of ripples in recirculating eddies, their spatial distribution, rotary migration patterns, and internal structure are given by *Rubin* [1987] and *Rubin et al.* [1990]. Flow velocities in areas of reattaching flow were measured using a two-channel electromagnetic current meter, sampling the longitudinal and cross-channel velocities once each second for durations as long

Table 1. Generalized Flow Conditions for Field and Laboratory Measurements

	Depth of Channel	Width of Channel, m	Main Stem velocity, m/s	Radius of Obstacle or Constriction, m	Reynolds Number
Colorado River	meters	100	1	10–100	10^6–10^7
Large flume	decimeters	4.0	1	2.5	10^5–10^6
Small flume	millimeters	0.15	0.1	0.016	10^2–10^3

as 24 hours. The time-varying location of the reattachment point was monitored by observing flags that were placed in the flow along the bank; the reattachment point was identified by locating the pair of adjacent flags with diverging orientations. In some experiments, flags were monitored at 15-min intervals for several hours, and in other experiments, flags were monitored continuously for durations of 1 hour. Precision of such measurements depends on flag spacing; for the 125-cm spacing used to collect the data reported here, precision is ±62.5 cm, which corresponds to less than ±5% of the maximum reattachment point excursion.

To insure that the observed eddy pulsations did not merely reflect unsteadiness of main stem flow, measurements were made at times when discharge was nominally steady (discharge from the upstream Glen Canyon Dam was regulated to be constant). Stage gauge data that were collected 100 km upstream and 40 km downstream from the current meter site (every 15 min) indicate that during the time of velocity measurement, main stem discharge was 240 m^3/s with a standard deviation of 2 m^3/s. During the time when the reattachment point location was monitored, stage gauge data (96 km upstream) indicate a mean discharge of 430 m^3/s with a standard deviation of 2 m^3/s. Generalized flow conditions for the field and laboratory flows are given in Table 1.

Two of the velocity time series were made using an electromagnetic current meter in a 30-m-long lateral separation eddy created in a 4-m-wide flume at the University of Tsukuba, Japan. One time series was collected 5 m downstream from the separation point, and one was collected near the reattachment point (22 m downstream from the separation point and 0.75 m from the sidewall). The flume was described by *Ikeda* [1983], and related lateral separation experiments using the same channel geometry were described by *Schmidt et al.* [1993].

Flow measurements were also made using a hot wire meter in a 15-cm-wide flume. Measurements were made in the lee of a cylinder (3.2 cm diameter for results presented here) that was isolated in the center of the flow in some experiments and adjacent to a sidewall or a flow-parallel plate in others. Three hundred time series were collected through the wakes and recirculation zones in these experiments, for a variety of flow conditions, cylinder diameters, and flow measurement locations. The time series were 1–30 min in duration and sampled at 20 Hz.

The flume that was developed for this work was built to maximize steadiness of flow. The pump was driven by a motor with a nominal speed accuracy of 0.2%. To minimize pump-induced vibration and pulsations, the entire pumping system was decoupled from the flume. Water was pumped into an isolated head tank where it was driven by gravity through a tube into a second head tank at the upstream end of flume. At the downstream end of the flume, water flowed through a tube into an isolated tail tank. All flow through the flume was driven by gravity; the pump transferred water from the tail tank to the upper of the two head tanks.

For the results presented in this paper, mean flow velocities (measured upstream from obstacles) were approximately 10 cm/s, standard deviations were less than 0.1 cm/s (1%), and maximum variations were ±0.2 cm/s (2%). It was necessary to insure such flow steadiness, so that observed unsteadiness of leeside flow could be attributed to intrinsic processes such as vortex shedding or self-organization of eddy recirculation rather than to variability of external forcing (unsteadiness of pumping or vibrations in the flume).

Spectral Analysis

Two kinds of data analysis techniques were applied to the time series that were collected during this study. Spectral analysis was used to search for periodicity, and nonlinear forecasting was used to search for deterministic nonperiodicity (chaos). Spectral analysis was performed using a fast Fourier transform algorithm. Each time series was divided into many equal-length pieces (using a Hann window); window length was chosen so that the pieces were long with respect to the vortex-shedding period. Using long pieces allows longer periodicity to be detected, and using multiple pieces allows confidence intervals to be determined for the power spectral calculations. The mean power at each frequency was computed by averaging the power of the individual pieces at that frequency. The 95% confidence limits were computed to be the mean value ± 2 standard deviations of the power calculated at each frequency.

Although spectral analysis is a useful technique for identifying structure in a time series, this technique can only identify structure that is periodic or linear. (A periodic signal is linear because the value x at any time t is a linear function of one or more preceding values. For example, a periodic sawtooth signal can be described by $x_t = -x_{t-1}$, and a sine curve can be described using a linear combination of two preceding values of x.) But a time series may contain a nonlinear structure in addition to linear structure, and spectral analysis cannot recognize such nonlinear structure. Nonlinear forecasting, discussed in the following section, is one technique for identifying nonlinear structure.

Nonlinear Forecasting

Several techniques have been developed recently to extract information about the nonlinear structure of a time series or spatial image [*Farmer and Sidorowich*, 1989; *Sugihara and May*, 1990; *Casdagli*, 1992; *Rubin*, 1992; *Theiler et al.*, 1992, 1994; *Casdagli and Weigend*, 1994]. The underlying principle of this time series forecasting is to predict future values of a time series by consulting a catalog of how the system evolved at other times when initial conditions were similar. Predictions are made by selecting an event (predictee) with a known history and known next value, searching the catalog for one or more events where the recent time history approximates the time history of the predictee, and then using the next values of these nearest neighbors in the catalog to predict the next value of the predictee. For some purposes, such as weather forecasting, financial forecasting, or noise reduction, predicting the future is the primary goal of the forecasting. In contrast, for the purpose of characterizing system dynamics, predictions are made to learn what kinds of models perform best.

The idea of relating a sequence of past values of a time series to the future is based on physical principles, not merely statistical convenience [*Packard et al.*, 1980; *Takens*, 1981]. The underlying principle is to use multiple values of a single variable as surrogates of many variables that may be required to define the initial state of a physical system for which the future is to be predicted. For example, a single value in a time series of velocity defines only the velocity, but two successive velocities define both velocity and acceleration.

The forecasting technique begins by splitting a time series into two pieces. One piece (a catalog or learning set) is used to relate the recent history of the series to the next value in the series. The other piece (testing set) is used to test the predictive ability of the catalog. In this forecasting process the recent history of the system for m steps through time (t) can be represented by a single point in m-dimensional space; the coordinates of that point are $(x_t, x_{t-1}, x_{t-2}, \cdots, x_{t+1-m})$. To make each prediction, a predictee sequence of m values in the time series is placed (or embedded) in this m-dimensional space, and the least squares method is used to identify the m-dimensional sequences in the learning set that are closest to the predictee. (This process of locating nearest neighbors is arithmetically equivalent to sliding the predictee sequence over a plot of the learning set time series and looking for the m-point sequences of the learning set that most closely match the predictee.) At least $m + 1$ of these nearest neighbors are located, so that least squares can be used to solve

$$x_{t+1} \approx \alpha_0 + \sum_{i=1}^{m} \alpha_i x_{t+1-i} \tag{1}$$

for the $m + 1$ coefficients $(\alpha_0, \cdots, \alpha_m)$ that best relate x_{t+1} to $x_t, x_{t-1}, x_{t-2}, \cdots, x_{t+1-m}$ in the learning set. The second step in making each prediction requires that (1) be solved again, this time substituting the coordinates of the predictee $(x_t, x_{t-1}, x_{t-2}, \cdots, x_{t+1-m})$ and the solved values for the coefficients $(\alpha_0, \cdots, \alpha_m)$. This second solution of (1) employs the relation determined from the learning set to predict x_{t+1} for the testing set.

Thus, to predict each point in the testing set requires that (1) be solved twice (first to learn the values of the coefficients that best relate the past to the future in the learning set, second to use those coefficients and the predictee sequence to predict the next value in the testing set). Each predicted value is then compared with the actual value in the testing set, and predictability is quantified either by the rms error of the predictions or by the correlation coefficient between predicted and observed values.

If the entire set of points in the learning set is used to evaluate the constants in (1), then the technique is a multiple linear regression, a classical statistical technique. In the newer nonlinear technique, a smaller number of (different) nearest neighbors in the learning set are used to reevaluate the constants $(\alpha_0, \cdots, \alpha_m)$ for each prediction, thereby allowing (1) to effectively model nonlinear relationships using small locally linear pieces.

One application of this approach is *Casdagli*'s [1992] deterministic-versus-stochastic forecasting technique, which measures forecasting error as a function of the number of neighbors (similar events) used to make predictions. At one extreme (stochastic linear modeling), forecasts are based on behavior learned from all events in a learning set. These global linear regression models maximize noise reduction but minimize sensitivity to the specific initial conditions for the event that is being forecast. At the other extreme (deterministic nonlinear modeling), forecasts are based on the relations learned from a small number of events for which the initial conditions are most similar to the event that is being forecast. In these nonlinear models, noise reduction is poorer, but sensitivity to initial conditions is enhanced. Casdagli argued that the dynamics of a system can be characterized by the class of model that makes the most accurate short-term forecasts. Low-dimensional nonlinear nonperiodicity (chaos) can be identified where nonlinear models employing a small number of nearest neighbors outperform global linear models.

Similarly, forecasting accuracy can be measured for models that vary the embedding dimension (m), to evaluate the number of active degrees of freedom of a system from which a time series was sampled. For example, m must be at least 3 to accurately forecast the behavior of a system with three degrees of freedom, such as *Lorenz*'s [1963] simplified model of convection. By applying forecasting in an exploratory manner (performing computations to evaluate the relative performance of a large number of models), the information contained within a time series can be used to evaluate the degrees of freedom, importance of nonlinearity, or other properties of a physical system [*Sugihara*, 1994]. Additional details of these modeling techniques are given by *Casdagli* [1992] and *Casdagli and Weigend* [1994]; the computational algorithm used in this study is a one-dimensional application of the two-dimensional (spatial) algorithm described by *Rubin* [1992].

The knowledge to be gained from these forecasting techniques can be compared to that gained from spectral analysis. Both techniques provide information about how a system operates, but not the specific equations that describe the system. Determining that a particular nonperiodic system is low dimensional or high dimensional, like determining the dominant frequencies of a periodic system, is merely a first step in characterizing or understanding the system.

Results

Field Observations

Longitudinal and cross-channel flow velocities were measured near the reattachment point on bars in the Colorado River. Typical hydraulic conditions can be approximated by a channel width of 100 m, a Reynolds of number 10^6–10^7, a flow depth of many meters, and an obstacle or constriction radius of tens or hundreds of meters (Table 1). Previous field measurements within lateral separation eddies have documented periodic vortex shedding near the separation point [*McDonald et al.*, 1994] or periodicity due to waves [*Bauer and Schmidt*, 1993], but our reattachment point time series are nonperiodic (Figure 2), as was the case for alongshore flow measured by *Bauer and Schmidt* [1993, Figure 7]; power at vortex-shedding frequencies (10^{-1} Hz) is orders of magnitude weaker than the low-frequency pulsations (Figure 2). Spectral analysis shows that the power in the reattachment point time series is inversely proportional to the square of the frequency, f. Power that decreases following this relation is characteristic of brown noise, which can be described as a running sum of uncorrelated numbers. The instantaneous location of the reattachment point (monitored using an array of flags that were placed in the flow along the bank) also lacks any demonstrable periodicity either in the time series (Figure 3) or power spectrum (not shown).

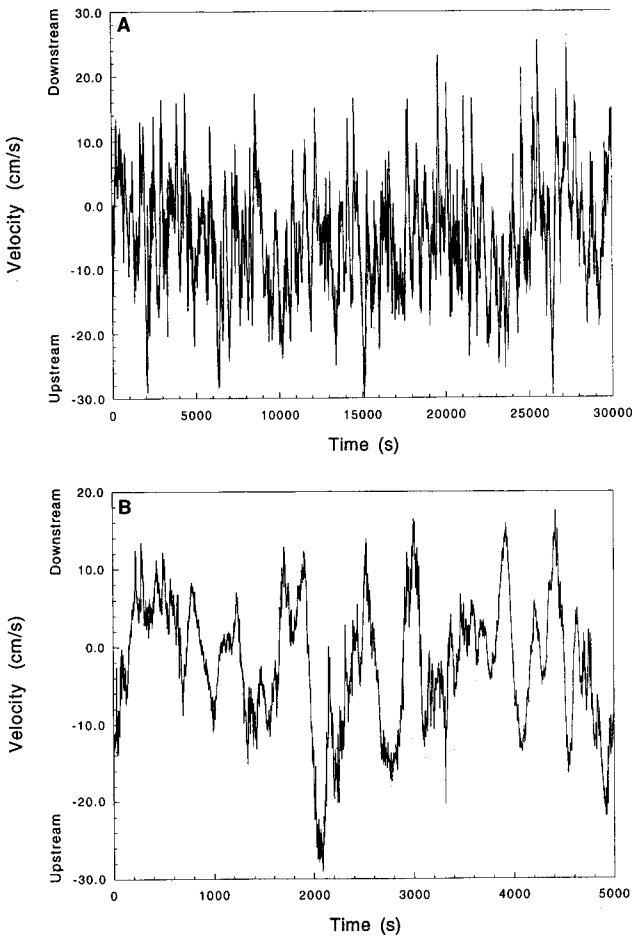

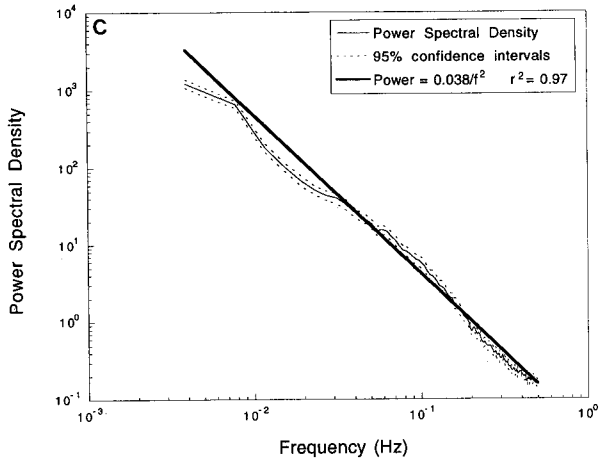

Figure 2. (continued)

Figure 2. Velocities measured near the reattachment point on a bar in the Colorado River in Grand Canyon, Arizona, October 22, 1990. Velocities were measured with an electromagnetic current meter sampling at 1 Hz; water depth was 1 m; current meter was 10 cm below the water surface. Location was 100 km downstream from Lees Ferry, Arizona; stage data that were collected every 15 min at sites 100 km upstream and 40 km downstream during a 3-day interval spanning the time of the velocity time series indicate that discharge was 240 m^3/s with a standard deviation of 2 m^3/s. (a) Plot of 30,000 s of the upstream-downstream component of velocity. The mean upstream-downstream component has a value of −4.7 cm/s, indicating that the current meter was slightly upstream from the time-averaged location of the reattachment point. (b) The first 5000 s of data in Figure 2a. (c) Power spectral density calculated from a 49,920-s time series subdivided into 195 subsets of 256 s. The thin solid line represents the mean power spectral density for all 195 subsets; dashed lines represent the 95% confidence interval, calculated from the distribution of power computed from the standard deviation of the 195 subsets; the thick line is a best fit line to illustrate that the power is inversely proportional to the square of the frequency f. Brown noise (a running sum of uncorrelated random numbers) has a power spectrum with this slope.

Lab Observations

Two kinds of laboratory experiments were conducted to investigate the conditions that produce nonperiodic eddy pulsations. In one set of experiments, hot wire measurements were made in the vortex street in the lee of an isolated cylinder and in the lateral separation eddy behind a cylinder placed alongside a flow-parallel plate (Figure 4). Flow depth was 0.6 cm, width was 15.0 cm, cylinder diameter was 3.2 cm, and the Reynolds number was 10^2–10^3 (Table 1). Where the cylinder was isolated in the flow, the character of vortex shedding varied with flow strength. In the slowest flows in which vortex shedding occurred, shedding was unstable and intermittent (Figure 5a). In slightly faster flows, vortex shedding became more regular (Figures 5b and 5c).

At Reynolds numbers lower than the range that we investigated (below approximately 10^2), flow in the lee of a cylinder takes the form of a pair of fixed eddies [*Batchelor*, 1967]. At the somewhat higher Reynolds numbers of our experiments (10^2–10^3), flow in the wake of an isolated cylinder is periodic, and power spectra are dominated by a peak at the vortex-shedding frequency (Figure 5b). This periodicity arises as vortices that are shed from the cylinder are advected downstream past the hot wire probe. When a plate is placed alongside the cylinder

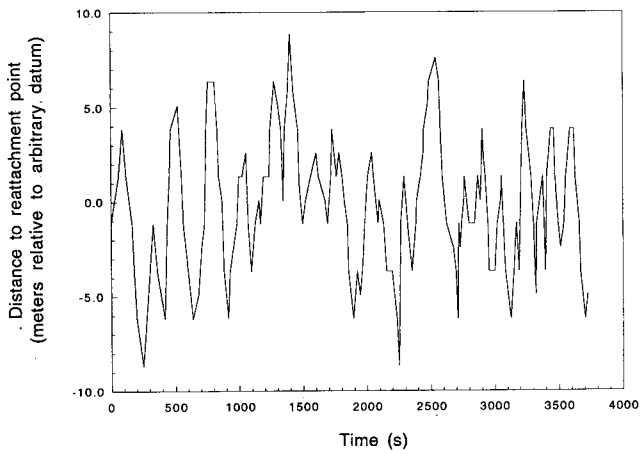

Figure 3. Plot showing the changing location of the reattachment point on a bar (196 km downstream from Lees Ferry, Arizona) in the Colorado River. Instantaneous reattachment point location was measured on May 22, 1991, using flags that were placed in the flow every 1.25 m along the bank. Release from Glen Canyon Dam (approximately 220 km upstream) was nominally steady, and stage gauge data indicate that discharge 96 km upstream from this field site was 430 m^3/s with a standard deviation of 2 m^3/s.

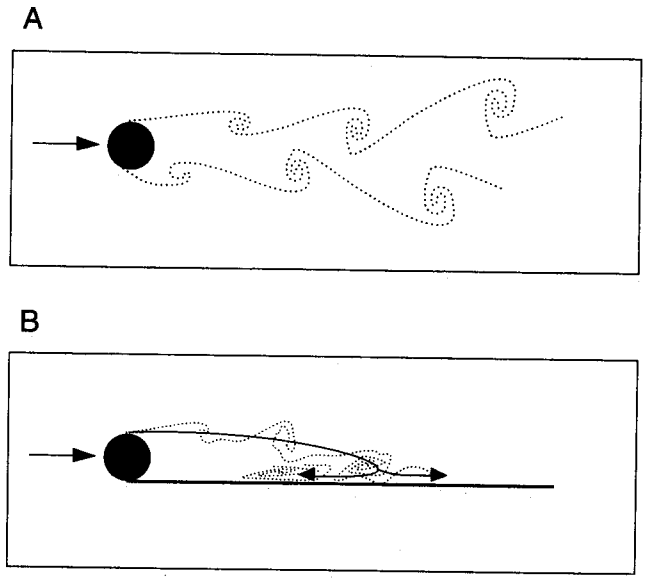

Figure 4. Experimental setup for small-flume experiments; flume, cylinder, and plate are drawn to scale, but vortex structure is schematic. Flume width was 15 cm; cylinder diameter was 3.2 cm; plate length was 30 cm.

(Figures 4 and 6), however, the character of the flow becomes grossly different, even if flow conditions are otherwise unchanged. Adding the plate causes the vortex street to be suppressed and produces a lateral separation eddy in the lee of the cylinder. Flow in the eddy is qualitatively similar to that in the river: The flow is nonperiodic (Figures 2 and 6).

The point of this experiment was not to model flow in the river with a small-scale analog. Rather, the point was to learn if the complexities in the field (high Reynolds number, complex geometry, or possible unsteadiness in main stem flow due to wind or other processes) are a necessary condition for eddies to pulsate irregularly. The results demonstrate that such complexities are not necessary; eddies pulsate irregularly even at a low Reynolds number in a steady flow with simple geometry.

The second experiment was conducted to look for spatial variability in flow character within a single recirculating eddy. Flow within an eddy in the 4-m-wide flume was measured near the separation and reattachment points. The time series collected near the separation point displays a periodic structure (Figure 7a), and the power spectrum has a broad peak at approximately 0.15–0.20 Hz, corresponding to a period of approximately 5–6 s, the period of vortex shedding observed during the experiment. This periodic vortex shedding occurs despite the irregular shape of the obstacle (pile of sandbags) along the sidewall of the flume. In the same main stem flow, however, flow near the reattachment point was nonperiodic (Figures 7b and 7c). The spatial difference is most clearly evident when the ratio of power in the two regions is considered (Figure 7d). At the vortex-shedding frequency, power near the separation point is almost an order of magnitude greater than near the reattachment point. In contrast, low-frequency power (representing nonperiodic pulsations) is greater near the reattachment point than at the separation point.

Discussion

Obstacle Geometry as a Cause of Nonperiodicity

These experiments demonstrate that nonperiodicity can be induced merely by a single change in obstacle geometry. Specifically, when a flow-parallel plate is placed alongside a cylinder, leeside flow can be induced to change from a periodic vortex street to an irregularly pulsating eddy (Figure 6). The higher Reynolds numbers, more complex geometry, and pos-

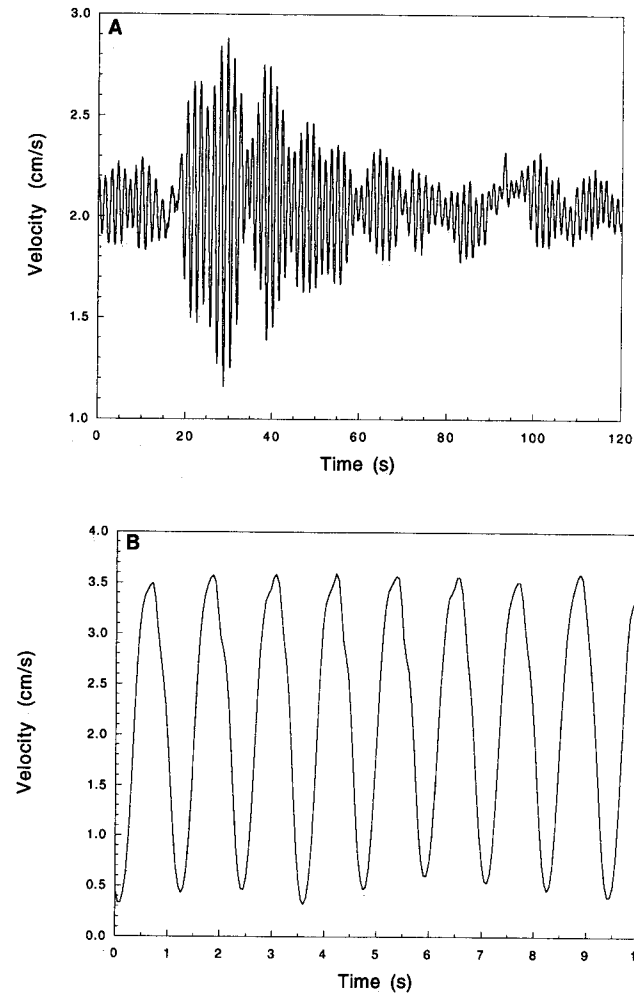

Figure 5. Hot wire velocity measurements and power spectra of flow in lee of a cylinder without a plate, as shown in Figure 4a. Velocities were measured at 20 Hz. (a) Intermittent vortex shedding at velocities just above the threshold for vortex shedding. Hot wire probe was positioned 7.2 cm downstream from the cylinder and 0.8 cm off axis. Flow depth was 0.6 cm; mean velocity at 0.3 cm above the bed was 9.7 cm/s (with no cylinder in flume). (b) Periodic vortex shedding. Depth was 0.6 cm; mean velocity at middepth upstream from the cylinder was 10.1 cm/s (standard deviation of 0.05 cm/s). Hot wire probe was positioned 7.0 cm downstream from the cylinder and 0.6 cm off axis; 10 s of a 2-min series. (c) Power spectral density of the complete time series in Figures 5a and 5b. The solid lines represent power spectral density; dashed lines represent the 95% confidence intervals. Spectral estimates for both time series were performed using a total series length of 2048 points (102.4 s) broken into 16 pieces of 128 samples. The velocity increase from Figure 5a to Figure 5b caused vortex shedding to become greater in power and higher in frequency.

sible unsteadiness of natural rivers, while perhaps contributing to flow variability, are not necessary for irregular eddy pulsations.

Flow Past a Cylinder Located Away From the Wall

Vortex shedding from cylinders occurs over a wide range of Reynolds numbers (approximately 5×10^1 to 10^4 according to *Batchelor* [1967] and *Schlichting* [1968]), but the process is most regular within the lower part of this range [*Roshko*, 1954; *Gaster*, 1969]. The frequency of vortex shedding, n, is given by

$$n = SU/d \tag{2}$$

where d is cylinder diameter, U is free stream velocity, and S is the dimensionless Strouhal number (nd/U). For the range of Reynolds numbers of the small-flume experiments (500 to 1000), the Strouhal number remains approximately constant at 0.2 [*Schlichting*, 1968].

Regularity of vortex shedding is also favored by two-dimensionality of the flow, for reasons that are explained by (2). Where an obstacle has differing diameters (such as cones studied by *Gaster* [1969]) different parts of the obstacle have different nominal shedding frequencies. Spanwise coupling between adjacent locations along the obstacle results in modulated pulses of vortices (increasing and decreasing amplitude), a phenomenon that Gaster observed in the lab and was able to model as a Van de Pol oscillator with a weak nonlinear term.

Just as shedding can be complicated by a spanwise gradient in diameter, Gaster hypothesized that differences in shedding frequency could also be induced by shear in the flow (a spatial gradient in velocity rather than obstacle diameter). It is not known whether the modulated vortex shedding observed in some of the small-flume experiments (Figure 5a) results from this process or from another instability.

Period doubling has been documented at the transition to chaos or turbulence in some previous studies of fluids [*Gollub et al.*, 1980; *Rockwell et al.*, 1991], but no period doubling was observed in these experiments. At some locations in the wake of the cylinder successive vortices were alternately strong and weak (Figure 6a). Although this behavior gave the appearance of period doubling (as might result from the pairing up of successive vortices [*Siggia and Aref*, 1980; *Cherry et al.*, 1984; *Rockwell et al.*, 1991]), in this case the alternations were caused by off-axis placement of the hot wire probe within the symmetrical wake. When the probe was placed near, but not exactly along, the axis of the wake, successive vortices were alternately weak and strong, depending on whether the vortex passing the probe had been shed from the near or far side of the cylinder. Thus these alternations in amplitude of successive vortices were not period doubling transitional with chaos.

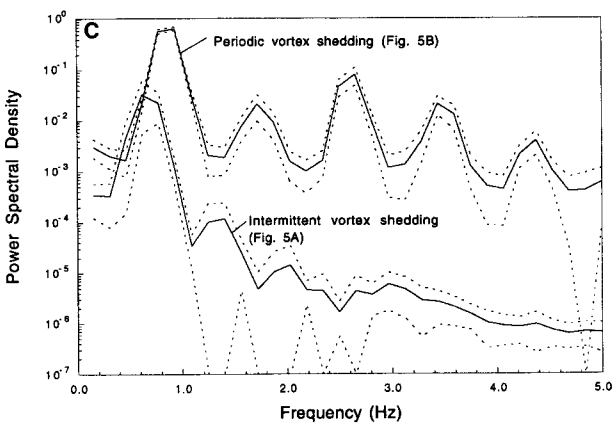

Figure 5. (continued)

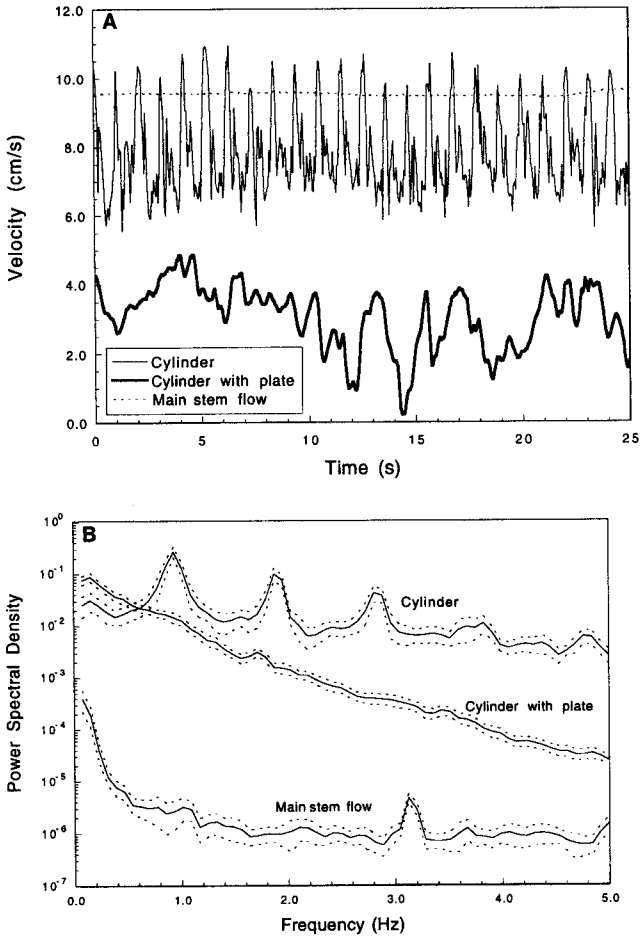

Figure 6. Effect of adding a plate adjacent to a cylinder. Except for addition of the plate, flow conditions were unchanged for these velocity time series. Without the plate, vortex shedding was periodic, with a fundamental frequency of approximately 1 Hz. When the plate was added, the system became nonperiodic. Mean location of the reattachment point on the plate was 16 cm downstream from cylinder. (a) Representative 25-s velocity time series of flow in the lee of an isolated cylinder and flow at the same location when the plate was placed alongside the cylinder. For both time series the hot wire probe was positioned 12.0 cm downstream from the cylinder and 0.5 cm off axis. Main stem flow (measured upstream from cylinder) is shown for comparison. Mean main stem velocity was 9.6 cm/s; standard deviation was 0.08 cm/s. (b) Power spectral density (with 95% confidence intervals) of the complete velocity time series in Figure 6a: 7.3 min without plate, 29 min with plate, and 7.1 min of main stem flow. The origin of the very weak peak at 3.2 Hz is unknown. All three time series were broken into 256-point (12.8-s) pieces for these power spectral calculations.

Flow Past an Obstacle Adjacent to a Wall

Experiments and computations have shown that the steadiness of some fluid processes varies with Reynolds number. For example, flow between rotating cylinders exhibits a variety of flow regimes that depend on Reynolds number [*Anderek et al.*,

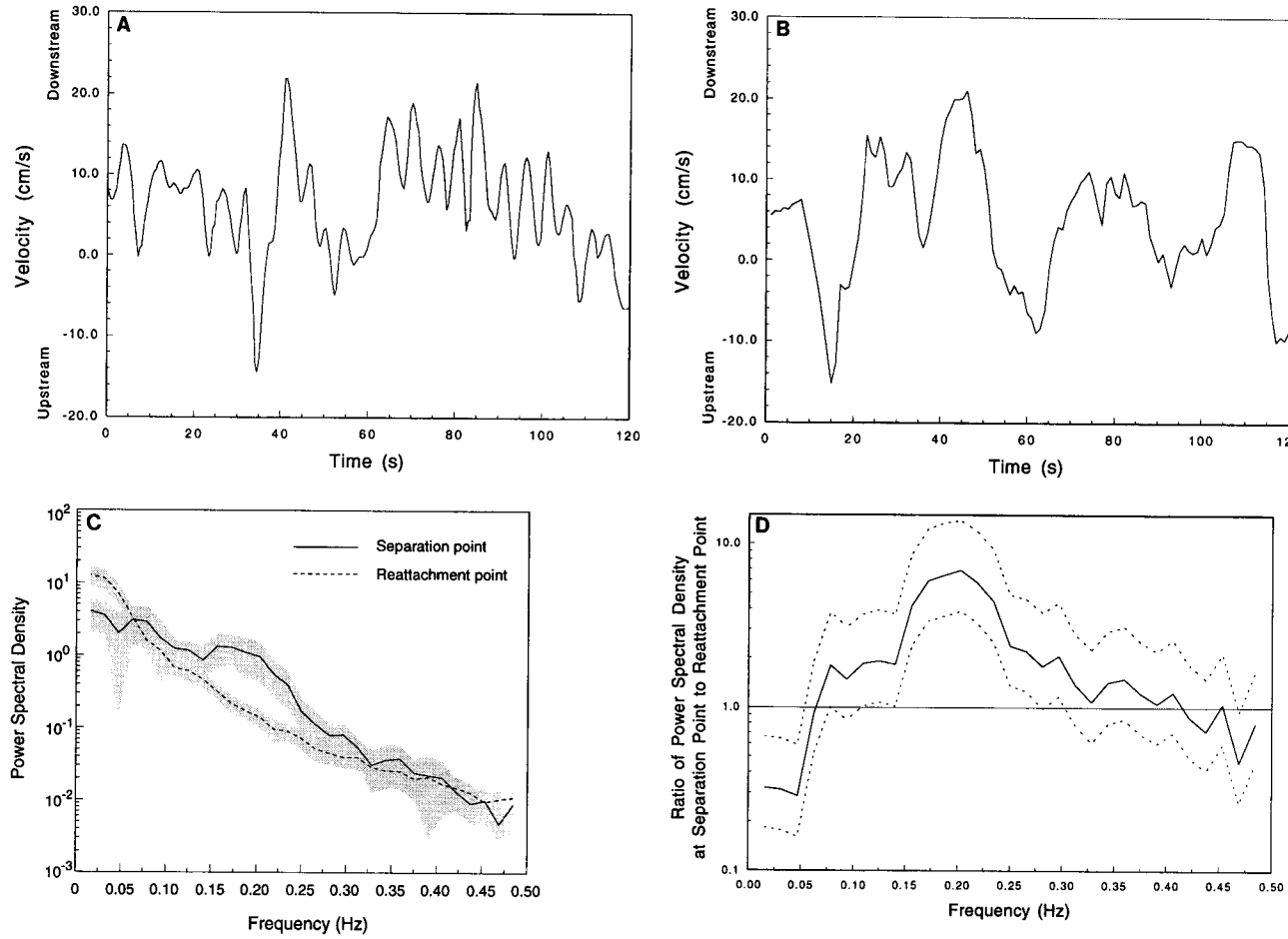

Figure 7. Electromagnetic current meter velocity time series and power spectral density measured in the 4-m-wide flume. (a) Time series collected at 1 Hz near the separation point (2 min from an 18-min record). Peaks represent the passage of vortices past the current meter. (b) Time series collected near the reattachment point (2 min from a 46-min record). (c) Power spectral densities of the complete time series from Figures 7a and 7b. Shaded areas represent the 95% confidence intervals. Near the separation point, vortex shedding was observed to occur with a mean period of approximately 6 s (0.17 Hz frequency). The power spectrum displays a relatively broad peak at this frequency. Near the reattachment point, the time series is less regular, and the power spectrum has no peak at the vortex-shedding frequency. For both curves of power spectral density, window size was 64 s. (d) Plot of the ratio of power at the separation point to power at the reattachment point. As the flow moves from the separation point to the reattachment point, vortex shedding decreases in power, while low-frequency pulsations gain power.

1986]. In our small-flume experiments, however, merely placing a plate alongside a cylinder is sufficient to cause the leeside flow to change from periodic to nonperiodic (Figure 6); the change from periodicity to nonperiodicity does not require a change in Reynolds number.

Where a cylinder is isolated in a flow, vortices that are shed from the cylinder are advected downstream, and only a small amount of recirculating fluid remains in the lee of the cylinder. Consequently, similar conditions recur after each vortex is shed. In contrast, where a cylinder is adjacent to a plate, a large recirculating eddy is trapped behind the cylinder, and similar conditions do not recur after each vortex is shed. Flow structures (pressure and momentum distribution in the recirculating flow) feed back through the recirculating flow to influence future flow in the eddy. Reattachment of flow structures such as vortices alters the reverse pressure gradient, which subsequently influences the strength of the recirculating flow [*Driver et al.*, 1987; *Simpson*, 1989]. Any such self-induced unsteadiness in the recirculating flow can be expected to feed back and affect the flow in the future, just as has been observed for recirculating flows that are artificially pulsed [*Simpson*, 1989]. The basic idea is that flow in the wake of the cylinder recirculates, thereby influencing future flow and future vortex shedding in the eddy [*Driver et al.*, 1987; *Simpson*, 1989]. In this regard, the process resembles simple mathematical models of chaotic systems such as convection rolls modeled by *Lorenz* [1963] or the periodically kicked rotor modeled by *Jensen* [1987]. In these mathematical models the future behavior of the system depends on the previous conditions (analogous to the pressure and momentum distribution throughout an eddy).

An additional complication in the recirculating eddy flow is that the wake interacts with the bank. As vortices are advected from the separation point toward the reattachment point, they deform and interfere with each other [*Cherry et al.*, 1984; *Simpson*, 1989], eventually becoming grossly deformed when they

impact the bank or sidewall. This deformation causes a reduction in periodicity (Figure 7).

This nonperiodicity of recirculating flow in lateral separation eddies is similar to results for flow over negative steps. *Simpson* [1989, p. 222] reported, "The period between flow reversals in the reattachment region appears to be random with no apparent correlation between the near-wall flow upstream and downstream of reattachment." This idea of randomness, however, appears to contradict the deterministic process whereby high-momentum structures in the wake "cause greater backflow at a later time" [*Simpson*, 1989, p. 223] (citing *Driver et al.* [1987]). One of the goals of the following section is to use nonlinear forecasting techniques to search for a deterministic structure in the eddy pulsation time series. If such a predictable structure could be demonstrated, the hypothesis of randomness could be falsified.

Nonperiodicity and Degrees of Freedom

At least three classes of systems can exhibit nonperiodic behavior: (1) high-dimensional (many degrees of freedom) linear systems, (2) low-dimensional nonlinear systems (chaos), and (3) high-dimensional nonlinear systems. Ideally, we would like to characterize nonperiodic eddy pulsations as one of these kinds of systems. In the first half of this century, *Landau* [1944] proposed that turbulence (nonperiodic flow) resulted from a large number of modes of excitation of a fluid (high-dimensional linearity), but in the last few decades, it has been shown theoretically and experimentally that some examples of nonperiodic flow are low-dimensional chaos [*Lorenz*, 1963; *Ruelle and Takens*, 1971; *Gollub and Swinney*, 1975; *Gollub et al.*, 1980]. The experimental studies that have documented low-dimensional chaos have focused on flows that are at the threshold of turbulence (transitional with laminar flow).

Several alternate explanations that do not involve low-dimensional chaos (spin glass relaxation, spatial noise amplification, and transients) have been proposed recently and are noted by *Crutchfield and Kaneko* [1988]. They argue that transient effects can dominate a system for long time intervals, and they therefore question the relevance of low-dimensional chaos to fully developed turbulence. As an example, they presented a computational example of a nonlinear system with a moderately high number of degrees of freedom (128). Their system eventually stabilizes to become periodic, but the time to attain periodicity is extremely long (10^{40} years, if iterations are performed at the rate of 10^{15} per second). For practical purposes the system is nonperiodic, despite the fact that it would theoretically become periodic.

The computational system described above has only a moderately high number of degrees of freedom. According to *Frisch and Orszag* [1990] the number of degrees of freedom of a turbulent fluid is given by $R^{9/4}$ per unit volume L^3, where R is the Reynolds number, and L is the length scale used to calculate R. For the Reynolds numbers and cylinder sizes in our experiments, the calculated number of degrees of freedom is of the order of 10^8. Although this relation may define the potential number of degrees of freedom in a fluid, the fluid may not actively employ all of them [*Gershenfeld and Weigend*, 1994].

Low-dimensional chaos (nonperiodicity with few degrees of freedom) such as the Lorenz system requires both low dimensionality (by definition) and nonlinearity (to allow nonperiodicity in a low-dimensional system). We used two forecasting techniques to evaluate the hypothesis that nonperiodicity in

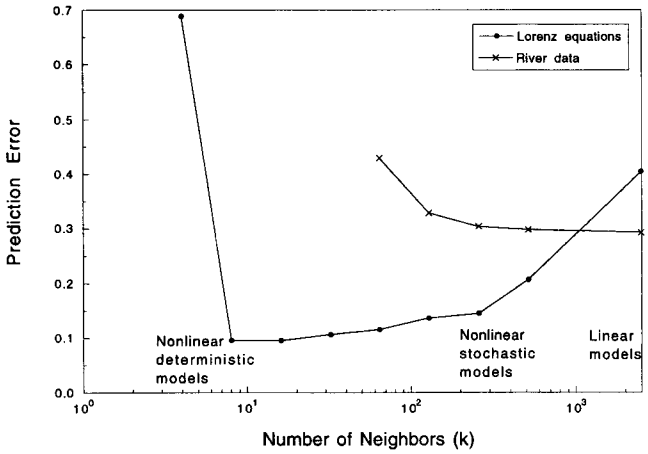

Figure 8. Plot showing rms prediction error as a function of the number of neighbors (k) used to make each prediction. Where k is small, forecasts are nonlinear and deterministic; where k is large, models are linear and/or stochastic [*Casdagli*, 1992]. The relative performance of these deterministic-versus-stochastic models can be used to infer properties of the system dynamics. Where minimum prediction errors are for models with low k, the system is deterministic and nonlinear (for example, the Lorenz equations). In contrast, where models with high k perform best (as is the case with eddy pulsations), the system is linear and/or stochastic. None of the eddy flows had the forecasting signature of nonlinear deterministic systems.

recirculating eddies (in the lab and in Grand Canyon) results from low-dimensional chaos. (More precisely, we attempted to falsify the null hypothesis that the observed flows were high-dimensional linear systems as proposed by *Landau* [1944].) First, we used the deterministic-versus-stochastic technique [*Casdagli*, 1992] to look for nonlinear structure in the time series. The best models (those with the lowest error) are purely linear (Figure 8), which does not contradict the hypothesis that this turbulence is linear.

The second technique is an attempt to determine the number of degrees of freedom of the lateral separation eddy. An upper limit to the number of active degrees of freedom can be estimated from model performance as a function of embedding dimension, or m in (1) [*Gershenfeld and Weigend*, 1994]. In the lateral separation eddy (Figure 6a) the best forecasting models employ an embedding dimension approaching 100, too high to support the idea of low-dimensional chaos. Thus this result fails to contradict Landau's hypothesis that turbulence is high-dimensional, and the deterministic-versus-stochastic technique fails to identify nonlinearity.

In some situations, low-dimensional chaos can be masked by stochastic effects such as noise or measurement error. In experiments with a computer-generated chaotic system, stochastic effects resulting from as little as 10% measurement error can be sufficient to mask low-dimensional dynamics [*Rubin*, 1992]. In the case of the data from recirculating flows in Grand Canyon, measurement error for the electromagnetic current meter is only a few percent, but we cannot rule out the possibility that the nonperiodicity results in part from system noise such as flow unsteadiness due to wind, waves, main stem flow pulsations caused by pulsations of upstream eddies, or other causes. In the case of the lab experiments, however, such effects are minimal. In this case, changing the obstacle geometry

(placing a plate adjacent to the cylinder) is sufficient to cause nonperiodicity to arise within the system. This nonperiodicity apparently results from high-dimensional processes rather than from low-dimensional nonlinearity.

Conclusions

1. For a wide range of experimental conditions, flow in the lee of an isolated cylinder is a periodic sequence of vortices. When a plate is placed adjacent to the cylinder, however, leeside flow takes the form of a lateral separation eddy that pulsates nonperiodically in size and velocity. These nonperiodic pulsations in recirculating flow arise spontaneously under steady forcing, just as periodic vortex shedding arises under steady forcing in the lee of an isolated cylinder.

2. Two processes are hypothesized to be responsible for the nonperiodic eddy pulsations. First, vortices and other flow structures in the wake of the cylinder are recirculated within the eddy and can alter the pressure and momentum distribution in the eddy, thereby influencing future circulation. Second, vortices that are shed from the cylinder become deformed as they impact and interfere with other deforming vortices.

3. Our computational techniques were unable to demonstrate that any of the nonperiodic flows result from low-dimensional nonlinear processes.

Acknowledgments. Rex Sanders (USGS) programmed the data logger for this work and helped with data collection in the field. Kristin Brown (USGS) helped with data collection in the field and lab. Hiroshi Ikeda provided use of the large flume at the University of Tsukuba; he and Jack Schmidt (Utah State) helped collect the data used for Figure 7. This manuscript was reviewed by Bruce Jaffe and Jon Nelson (both USGS) and by Jack Schmidt (Utah State). This work was funded in part by the Glen Canyon Environmental Studies program and in part by a USGS G. K. Gilbert Fellowship.

References

Anderek, C. D., S. S. Liu, and H. L. Swinney, Flow regimes in a circular Couette system with independently rotating cylinders, *J. Fluid Mech.*, *164*, 155–183, 1986.

Andrews, E. D., Deposition rate of sand in lateral separation zones, Colorado River, (abstract), *Eos Trans. AGU*, *72*(44), Fall Meeting suppl., 219, 1991.

Batchelor, G. K., *An Introduction to Fluid Dynamics*, Cambridge University Press, New York, 1967.

Bauer, B. O., and J. C. Schmidt, Waves and sandbar erosion in the Grand Canyon: Applying coastal theory to a fluvial system, *Ann. Assoc. Am. Geogr.*, *83*, 475–497, 1993.

Casdagli, M., Chaos and deterministic versus stochastic nonlinear modeling, *J. R. Stat. Soc. B*, *54*, 303–328, 1992.

Casdagli, M., and A. S. Weigend, Exploring the continuum between deterministic and stochastic modeling, in *Time Series Prediction: Forecasting the Future and Understanding the Past*, edited by A. S. Weigend and N. A. Gershenfeld, pp. 347–366, Addison-Wesley, Reading, Mass., 1994.

Cherry, N. J., R. Hillier, and M. P. Latour, Unsteady measurements in a separated and reattaching flow, *J. Fluid Mech.*, *144*, 13–46, 1984.

Crutchfield, J. P., and K. Kaneko, Are attractors relevant to turbulence?, *Phys. Rev. Lett.*, *60*, 2715–2718, 1988.

Davies, D. K., Sedimentary structures and subfacies of a Mississippi River point bar, *J. Geol.*, *74*, 234–239, 1966.

Driver, D. M., H. L. Seegmiller, and J. Marvin, Time-dependent behavior of a reattaching shear layer, *AIAA J.*, *25*, 914–919, 1987.

Farmer, J. D., and J. J. Sidorowich, Exploiting chaos to predict the future and reduce noise, in *Evolution, Learning, and Cognition*, edited by Y. C. Lee, World Scientific, River Edge, N. J., 1989.

Frisch, U., and S. A. Orszag, Turbulence: Challenges for theory and experiment, *Phys. Today*, *43*, 24–32, 1990.

Gaster, M., Vortex shedding from slender cones at low Reynolds numbers, *J. Fluid Mech.*, *38*, 565–576, 1969.

Gershenfeld, N. A., and A. S. Weigend, The future of time series: Learning and understanding, in *Time Series Prediction: Forecasting the Future and Understanding the Past*, edited by A. S. Weigend and N. A. Gershenfeld, pp. 1–70, Addison-Wesley, Reading, Mass., 1994.

Gollub, J. P., and H. L. Swinney, Onset of turbulence in a rotating fluid, *Phys. Rev. Lett.*, *35*, 927–930, 1975.

Gollub, J. P., S. V. Benson, and J. Steinman, A subharmonic route to turbulent convection, in Nonlinear Dynamics, edited by R. H. G. Helleman, *Ann. N. Y. Acad. Sci.*, *357*, 22–27, 1980.

Ikeda, H., Experiments on bedload transport, bed forms, and sedimentary structures using fine gravel in the 4-meter-wide flume, *Environ. Res. Cent. Pap.*, *2*, Univ. of Tsukuba, Ibaraki, Japan, 1983.

Jensen, R. V., Classical chaos, *Am. Sci.*, *75*, 168–181, 1987.

Landau, L. D., Turbulence, *Dokl. Akad. Nauk SSSR*, *44*(8), 339–342, 1944.

Leeder, M. R., and P. H. Bridges, Flow separation in meander bends, *Nature*, *253*, 338–339, 1975.

Leopold, L. B., R. A. Bagnold, M. G. Wolman, and L. M. Brush, Flow resistance in sinuous or irregular channels, *U.S. Geol. Surv. Prof. Pap.*, *282-D*, 111–134, 1960.

Lorenz, E. N., Deterministic nonperiodic flow, *J. Atmos. Sci.*, *20*, 130–141, 1963.

McDonald, R. R., J. M. Nelson, E. D. Andrews, D. H. Campbell, and D. M. Rubin, Field study of the mechanics of flow in lateral separation eddies in the Colorado River (abstract), *Eos Trans. AGU*, *75*(44), Fall Meeting suppl., 268, 1994.

Nelson, J. M., Experimental and theoretical investigation of lateral separation eddies (abstract), *Eos Trans. AGU*, *72*(44), Fall Meeting suppl., 218–219, 1991.

Nelson, J. M., R. R. McDonald, and D. M. Rubin, Computational prediction of flow and sediment transport patterns in lateral separation eddies (abstract), *Eos Trans. AGU*, *75*(44), Fall Meeting suppl., 268, 1994.

Packard, N. H., J. P. Crutchfield, J. D. Farmer, and R. S. Shaw, Geometry from a time series, *Phys. Rev. Lett.*, *45*, 712–716, 1980.

Rockwell, D., F. Nuzzi, and C. Magness, Period doubling in the wake of a three-dimensional cylinder, *Phys. Fluids A*, *3*, 1477–1478, 1991.

Roshko, A., On the development of turbulent wakes from vortex streets, *Natl. Advis. Comm. Aeronaut. Rep.*, *1191*, 1954.

Rubin, D. M., *Cross-Bedding, Bedforms, and Paleocurrents*, 187 pp., Society of Economic Paleontologists and Mineralogists, Tulsa, Okla., 1987.

Rubin, D. M., Use of forecasting signatures to help distinguish periodicity, randomness, and chaos in ripples and other spatial patterns, *Chaos*, *2*, 525–535, 1992.

Rubin, D. M., J. C. Schmidt, and J. N. Moore, Origin, structure, and evolution of a reattachment bar, Colorado River, Grand Canyon, Arizona, *J. Sediment. Petrol.*, *60*, 982–991, 1990.

Ruelle, D., and F. Takens, On the nature of turbulence, *Commun. Math. Phys.*, *20*, 167–192, 1971.

Schlichting, H., *Boundary-Layer Theory*, 817 pp., McGraw-Hill, New York, 1968.

Schmidt, J. C., Recirculating flow and sedimentation in the Colorado River in Grand Canyon, Arizona, *J. Geol.*, *948*, 709–724, 1990.

Schmidt, J. C., and J. B. Graf, Aggradation and degradation of alluvial sand deposits, 1965 to 1986, Colorado River, Grand Canyon National Park, Arizona, *U.S. Geol. Surv. Prof. Pap.*, *1493*, 1990.

Schmidt, J. C., D. M. Rubin, and H. Ikeda, Flume simulation of recirculating flow and sedimentation, *Water Resour. Res.*, *29*, 2925–2939, 1993.

Shipek, C. J., Photographic survey of sea floor on southwest slope of Eniwetok Atoll, *Geol. Soc. Am. Bull.*, *73*, 805–812, 1962.

Siggia, E. D., and H. Aref, Scaling and structures in fully turbulent flows, in Nonlinear Dynamics, edited by R. H. G. Helleman, *Ann. N. Y. Acad. Sci.*, *357*, 368–376, 1980.

Simpson, R. L., Turbulent boundary-layer separation, *Annu. Rev. Fluid Mech.*, *21*, 205–234, 1989.

Smith, J. D., and S. M. Wiele, Exchange of sand between the bed and margins of rivers with perimeters composed predominantly of gravel and bedrock (abstract), *Eos Trans. AGU*, *75*(44), Fall Meet. suppl., 269, 1994.

Sugihara, G., Nonlinear forecasting for the classification of natural

time series, *Philos. Trans. R. Soc. London A*, *348*(1688), 477–495, 1994.

Sugihara, G., and R. M. May, Nonlinear forecasting as a way of distinguishing chaos from measurement error in time series, *Nature*, *344*, 734–741, 1990.

Takens, F., Detecting strange attractors in turbulence, in *Dynamical Systems and Turbulence*, edited by D. Rand and L. Young, pp. 366–381, Springer-Verlag, New York, 1981.

Theiler, J., B. Galdrikian, A. Longtin, S. Eubank, and J. D. Farmer, Using surrogate data to detect nonlinearity in time series, in *Nonlinear Modeling and Forecasting*, edited by M. Casdagli and S. Eubank, pp. 163–188, Addison-Wesley, Reading, Mass., 1992.

Theiler, J., P. S. Linsay, and D. M. Rubin, Detecting nonlinearity in data with long coherence times, in *Time Series Prediction: Forecasting the Future and Understanding the Past*, edited by A. S. Weigend and N. A. Gershenfeld, pp. 429–455, Addison-Wesley, Reading, Mass., 1994.

Yeh, H. H., W. Chu, and O. Dahlberg, Numerical modeling of separation eddies in shallow water, *Water Resour. Res.*, *24*, 607–614, 1988.

R. R. McDonald, U.S. Geological Survey, Mail Stop 413, Denver Federal Center, P. O. Box 25046, Lakewood, CO 80225-0046.

D. M. Rubin, U.S. Geological Survey, Mail Stop 999, 345 Middlefield Road, Menlo Park, CA 94025.

(Received June 20, 1994; revised January 17, 1995; accepted February 2, 1995.)